

# THERMODYNAMICS AND KINETICS OF VAPORIZATION OF PbS FROM COMPLEX Cu-Fe MATTES

K. Sadrnezhaad

Department of Metallurgical Engineering  
Sharif University of Technology  
Tehran, Iran

**Abstract** Thermodynamics and kinetics of vaporization of lead sulfide from typical copper-smelting mattes of commercial interest are investigated in the temperature range 1388 K to 1573 K by vapor transport technique and plasma arc spectroscopy. The total mass of the dominant vaporizing species PbS that leaves the matte is described by the Newman's numerical solution to the second Fick's law combined with the experimental boundary conditions of the system. This solution is obtained through the application of the Laplace transform series expansion method stated by Crank. The three steps that are used to describe the rate of vaporization of PbS are: the diffusive transport of PbS through the liquid phase, the equilibrium at the gas-matte interface and the diffusion through the stagnant layer of gas above the surface of the melt. With the particular experimental set-up and the condenser weight gain, it is shown that the activity coefficient of PbS is simply a function of the temperature and the composition of the bearing phase. The enthalpy and the entropy of dissolution of PbS in hot liquid mattes are estimated to be respectively -41 KJ/mol and 20 to 40 J/mol.K depending on the temperature and the composition of the liquid mattes of this investigation.

**Key words** Kinetics, Vaporization, Lead, PbS, Matte, Transportation Method, Activity Coefficient, Dissolution, Entropy, Enthalpy

**چکیده** ترمودینامیک و سینتیک تبخیر سولفید سرب از ماتهای صنعتی تولید مس در محدوده دماهای ۱۳۸۸ تا ۱۵۷۳ درجه کلوین از طریق انتقال بخار و اسپکتروسکوپی قوس پلازما در این مقاله بررسی شده است. مجموع جرم جزء تبخیر شونده اصلی یعنی PbS از طریق حل قانون دوم فیک همراه با شرایط مرزی بدست می آید. برای اینکار از حل عددی «نیومن» و روش بسط سری تبدیل لاپلاس که توسط «کرنک» تشریح شده، استفاده می شود. تبخیر PbS مشتمل بر سه مرحله زیر است: نفوذ PbS در فاز مایع، تعادل در فصل مشترک گاز با مات و نفوذ در لایه ایستای گاز بالای سطح مذاب. افزایش وزن میرد نشان می دهد که ضریب اکتیویته سولفید سرب تابع دما و غلظت فاز مذاب است. انتالپی و انتروپی انحلال سولفید سرب در ماتهای این تحقیق برترتیب ۴۱- کیلوژول بر مول و ۲۰ تا ۴۰ ژول بر مول بر کلوین تخمین زده می شود. این مقادیر تابع دما و غلظت فاز مات است.

## INTRODUCTION

Copper-smelting systems usually produce around 2.5 tons of molten matte for each ton of blister copper. This matte contains up to 5 percent of heavy metal impurities such as lead, zinc and tin. These metals are encountered in increasing concentrations in both copper concentrates and scraps which are the feed materials for the smelters.

Due to their high volatility, the impurity elements may be carried in sulfide, oxide and/or metallic forms with the off-gases from smelting and converting

furnaces. They are potentially hazardous because they can condense and choke the dust-cleaning systems of the smelters and/or converters. They may also leak into the environment with the fugitive emissions of the furnaces.

The elimination, recovery and reduction of impurity elements from smelting and converting copper mattes depend upon the provision of precise thermodynamic and kinetic information on their vaporization process from complex Cu-Fe mattes. Knowledge of the mechanisms of evolution of the residual species is an important element of any investigation

on the ways (a) to diminish the potential harm to the environment, (b) the methods for improving the smelter and converter operations and (c) the procedures for extracting possible metallic by-products from copper-making systems.

Complex molten mattes are less understood than most other phases of practical interest. Vaporization of the residual species from these systems depends, however, on their thermodynamic and kinetic properties and conditions [1,2]. While thermodynamic information is scarce and greatly dispersed, there is virtually no kinetic information available on the vaporization of most residual species from these phases.

The information available on the activity of PbS is, for example, restricted to a few high copper sulfide mattes [3,4,5,6]. Because of the difficulties usually encountered working with these phases, the published data are extremely scattered. PbS activity coefficients of 0.13 [3], 2.4[4], 0.035 [7] and 0.166 [8] are, for example, obtained from the studies on dilute sulfides of similar conditions. It is said that the discrepancies are related to the extrapolation of the lower concentrations of the activity data [8]. It seems, however, that the crucial reason rests upon the failure of the experimental systems used by some of the previous researchers to assure equilibrium between the gas and the melt.

From a thermodynamic point of view, the emissions from hot liquid mattes carrying a few percent lead may contain Pb, PbS,  $Pb_2S_2$  and  $S_2$ . However mass-spectrometric measurements have shown that at the experimental temperatures of 979 to 1182 K the predominant component emitted is PbS [9]. Based on the extrapolation of such information, it has been deduced that PbS is the predominant fugitive emission to evolve from a lead bearing sulfide at higher temperatures of smelting and converting furnaces [7].

Matte compositions in many smelter and con-

verter samples show a lead content of around 0.9 to 2.6 weight percent. This indicates a PbS mole fraction of 0.005 to 0.015 in a typical pseudo-ternary  $Cu_2S$ -FeS-PbS system. However, the matte contents used by many investigators are far greater than this value [3, 4,5,7]. The mole fraction of PbS in the pseudo-ternary  $Cu_2S$ -FeS-PbS mattes used at 1473 K by Eric and Timucin [7] has been larger than 0.20; in the pseudo-binary  $Cu_2S$ -PbS system used by Azuma, et al., [4], it has been greater than 0.06; and in the pseudo-ternary  $Cu_2S$ -FeS-PbS system used by Nesterov, et al., [3], it has been greater than 0.076.

It has previously been shown that the extrapolation of the lower concentration of constituent activities in the  $Cu_2S$ -FeS-PbS system can lead to the misleading results [8]. This can also be shown to be true for higher concentrations where the validity of Henry's law is not justified. The matte compositions used by Sinha, et al., [8] and Roine and Jalkanen [10,11] have been in the very low ranges of less than 0.009 and 0.002 mole fractions PbS. Their results must, therefore, be attributed to the infinitely dilute solutions and cannot be used for higher concentrations. The chemical composition of the samples used in this study covers the range of 0 to 3 mass % PbS, up to 56 mass% FeS and 41 to 97 mass%  $Cu_2S$ .

The only information available on the kinetics of vaporization of PbS is that of El-Rahaiby and Rao [12]. Their results indicate considerable influence for both pore-diffusion and chemical reaction when PbS is vaporized from solid mixtures used for direct reduction of PbS. Their study is limited to the vaporization of PbS from solid PbS/4 CaO samples in the temperature range 1058 K to 1196 K. Because of considerable differences in the composition and the state of the samples, their findings are not applicable to higher temperatures where most mattes are homogeneous molten liquids.

The purpose of this study is to contribute to the limited amount of information available on the

thermodynamics and kinetics of vaporization of lead sulfide from complex Cu-Fe mattes of various chemical compositions. A combined thermodynamics versus kinetics approach is utilized here to remedy the undesirable problems usually encountered with transitional vapor-pressure techniques [1,2].

## EXPERIMENTS

Synthetic mattes are made of carefully mixed -200, -100 and -100 mesh  $\text{Cu}_2\text{S}$ ,  $\text{FeS}$  and  $\text{PbS}$  (99.999, 99.9 and 99.45 mass % pure) powders, respectively. Each sample is held in an alumina boat which, in turn, rests in a larger carrier boat. The carrier boat is placed inside the reaction chamber and is heated radiationally. The reaction chamber is a 90 cm long, 3.6 Cm I.D. alumina tube that is enclosed in a horizontal tube furnace that is heated by four silicon-carbide elements. The reaction chamber includes a hot zone of at least 5 times the length of the carrier boat.

High purity argon (99.999%) is passed over reduced copper screen and  $\text{H}_2\text{O}/\text{CO}_2$  absorption column. The flow rate of the gas is controlled with a constant-head capillary flow-meter. In order to obtain a well defined oxygen pressure in the gas, pure iron powder is placed before the vaporization zone of the reaction tube. A semi-cylindrical ceramic insert is placed upstream from the matte sample to develop a well defined flow of gas over the sample.

To diminish the loss of heat at the inlet and outlet of the reaction tube, appropriate insulations are used at both ends of the furnace. The exception is for the water-cooled copper cap which receives the enthalpy of condensation of the vaporized substances. The temperature profile inside the furnace is so that the maximum temperature is between the sample and the condenser finger. Careful examination of the surface of the reaction chamber indicates no condensation on the interior of the chamber.

The furnace temperature is maintained within

$\pm 2^\circ\text{C}$  during a test. This is done both manually and thermostatically by hand manipulation of the voltage regulator of the furnace. A precise calibration of the temperature readings is made by means of a separate Pt/Pt-Rh thermocouple whose bead is positioned at the middle of the region where the carrier boat is placed. Measurements show that there is no considerable temperature error and that the experimental figures are reproducible.

Before each experiment, the copper screen is reduced with commercially pure hydrogen for at least one hour and the whole assembly is purged with purified argon for at least thirty minutes. Condensation front is covered with a thin foil of aluminum wrap whose weight is about 0.8 grams. After receiving the volatile species of the gas, the wrap is removed and re-weighed. The captured deposit is then dissolved in hot nitric acid. This is done by dipping and then flushing the covered part of the wrap into 25  $\text{cm}^3$  of 3 mol/liter  $\text{HNO}_3$  at  $67^\circ\text{C}$ . Experiments show that fresh deposits dissolve faster.

The complete dissolution of the deposit by this process usually takes 30 to 60 minutes. The stabilization of the mixture, however, needs a much longer time during which the solution must be kept warm. The aqueous solution is diluted to 100  $\text{cm}^3$  and analyzed by a DC plasma arc elemental emission spectrometer. The analysis is repeated several times and the average is utilized for mathematical calculations.

Blank measurements indicate that the weight change of the uncovered wrap is not considerable. A comparison of the total gains in the weights of the wraps with the total loss in the weight of the boat in the same experiment shows that there is an almost fixed difference between the two. This difference can be attributed to the vaporization of the non-condensable species such as moisture, plus the reduction of the boat under highly purified argon atmosphere.

Corrections are made for escape of the gas during

the replacement of the wrap. The corrected weight-gain between  $i^{\text{th}}$  and  $i+1^{\text{th}}$  readings is thus, by simple arithmetic:

$$\Delta W_c = \Delta W_m \frac{t_{i+1} - t_i}{(t_{i+1} - t_i) - \Delta t} \quad (1)$$

where  $\Delta W_m$  is the measured weight gain,  $t$  is the time and  $\Delta t$  is the time difference for removing the wrap. These corrections have in no case been more than 5 percent.

The weight losses of the samples are seen systematically consistent with the weight gains of the finger. Any resistance due to the deposition on the surface of the finger can simply be ignored due to the large contact area and sharp temperature drop here.

The initial weight of all samples is 5 grams. The greatest condenser weight gain for 3 hours of continued vaporization is 0.21 grams. This weight gain is due to the condensation of different components of the gas, as shown by:

$$\Delta W_t = \Delta W_{PbS} + \Delta W_{Pb} + \Delta W_{Pb_2S_2} + \Delta W_{S_2} + \Delta W_R \quad (2)$$

$\Delta W_t$  is the total weight gain,  $\Delta W_{PbS}$ ,  $\Delta W_{Pb}$ ,  $\Delta W_{Pb_2S_2}$  and  $\Delta W_{S_2}$  are contributions of the corresponding components and  $\Delta W_R$  is the weight gain for other residual impurities and substances.

The vaporization experiments are performed at eight different temperatures between 1388 K and 1573 K under argon atmosphere. The base-compositions of the mattes are selected along  $Cu_2S$ - $FeS$  binary in the  $Cu$ - $Fe$ - $S$  system (Figure 1). They consist of up to 2.6 percent lead as the forth constituent (Table I). From the liquidus temperatures demonstrated in Figure 1, it is obvious that except one matte which is kept at the liquid/solid mushy region, all the other mattes are homogeneous liquids with different superheats at the temperatures of the experiments. An example is matte III in which the amount of the superheat

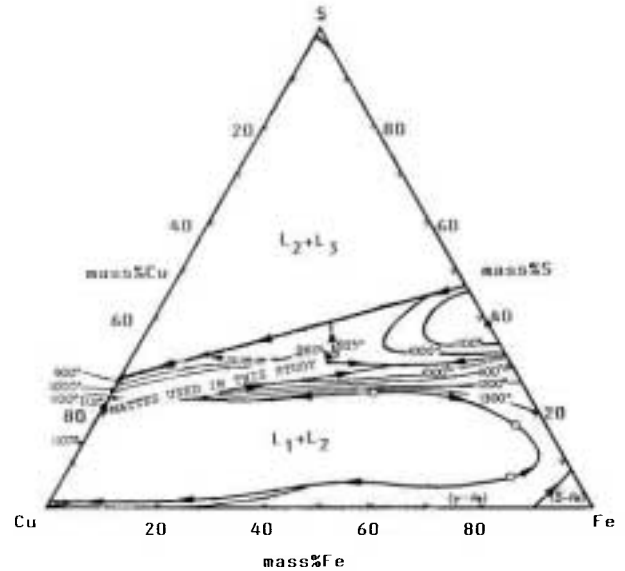


**Figure 1.** The liquidus in  $Cu$ - $Fe$ - $S$  system [13] and the base-composition of the mattes used in this investigation.

differs from a small value of  $\sim 120^\circ C$  at  $1140^\circ C$  to a relatively large amount of  $\sim 280^\circ C$  at  $1300^\circ C$ . Since the evolution rates of the gases may depend on the amount of the superheat, it may be worth while to study this effect.

## RESULTS

Various mattes of Table I are extracted to determine

**TABLE I.** Initial Composition of the Mattes.

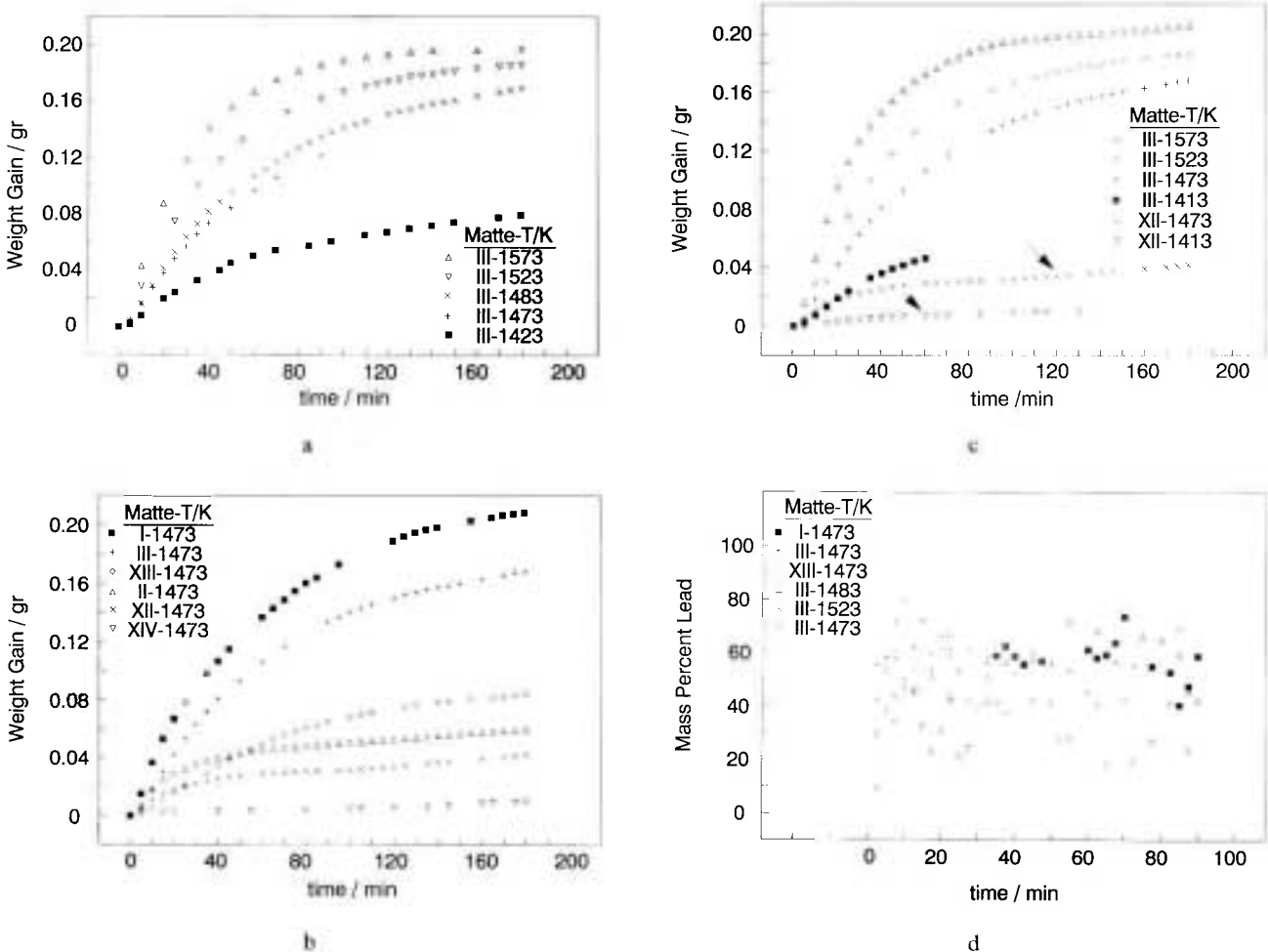
Matte	mass% Pb	mass% Cu	mass% Fe	mass% S
I	2.60	32.80	35.64	28.96
II	nil	33.84	36.72	29.44
III	2.60	44.80	26.09	26.51
IV	2.08	45.07	26.25	26.59
V	1.65	45.30	26.38	26.66
VI	1.39	45.43	26.46	26.70
VII	0.95	45.67	26.60	26.76
VIII	0.78	45.76	26.65	26.79
IX	2.50	45.20	26.30	25.90
X	2.56	44.78	26.08	26.50
XI	1.08	45.50	26.49	26.92
XII	nil	46.16	26.92	26.92
XIII	2.60	77.60	nil	19.80
XIV	nil	80.00	nil	20.00

the effect of time and temperature on weight and composition of the vaporized materials. Sample examples are demonstrated in Figure 2 in which typical results are given for different boats. Re-extraction tests are performed for two mattes of the same composition at different temperatures specified in the figure. The arrows indicate the starting time of the re-extraction tests. These tests are carried out on frozen samples initially melted, subsequently vaporized and finally cooled-off while remained in the same carrier boat. The purpose of the re-extraction tests is to determine the influence of the initial physical charac-

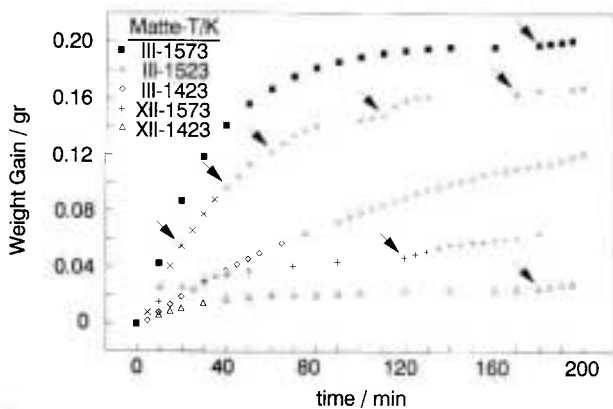
teristics of the mattes on the vaporization process.

Figure 3 shows several more re-extraction results. Mathematical manipulation of these results indicates that the activity coefficients obtained from the extraction of the solid frozen samples are comparable with those obtained through the extraction of the mixed sulfide powders. This proves that the pull-out solidification of the melt produces similar homogenization effect as that caused by the mixing of the powders.

From analyses and the total weight gain results, the total amount of PbS vaporized from different



**Figure 2.** Typical weight gain results (a, b and c) and analyses (d) of condensed materials evaporated from binary and ternary mattes with compositions given in Table I. (a)  $L_1=0.36$  cm,  $L_2=0.60$  cm; (b and c)  $L_1=0.26$  cm,  $L_2=0.76$  cm. For illustration of  $L_1$  and  $L_2$ , see Figure 5.



**Figure 3.** Effect of the homogenization due to pull-out solidification on the total weight of the species vaporized from different mattes. The arrows point to the times at which the pre-extraction experiments are ceased.

mattes of this investigation is determined and used to calculate the fractional weight of the lead sulfide, as defined by Equation 3:

$$F_{\text{PbS}} = \frac{(W_{\text{PbS}})_t}{(W_{\text{PbS}})_\infty} \quad (3)$$

where  $(W_{\text{PbS}})_t$  and  $(W_{\text{PbS}})_\infty$  are the weights of PbS vaporized up to  $t = t$  and  $t = \infty$ , respectively. A sample example of the fractional weight gain is demonstrated in Figure 4.

A schematic representation of the vaporization system is provided in Figure 5. It is assumed that the rates of vaporization of components other than PbS are negligible [7]. The species PbS must diffuse first through the melt towards the matte-gas interface, i.e.  $y = L_1$ , and then through the stagnant layer of gas filling the upper empty part of the boat extending from  $Y = L_1$  to  $y = L_2$ .

Several tests are conducted to determine the effect of the geometry of the samples as compared to that of the reaction tube. Observations show that with the present geometry, the rate of flow of argon do not affect the vaporization rate. An example is shown in Figure 6 in which the total mass of the species vaporized from Matte III of

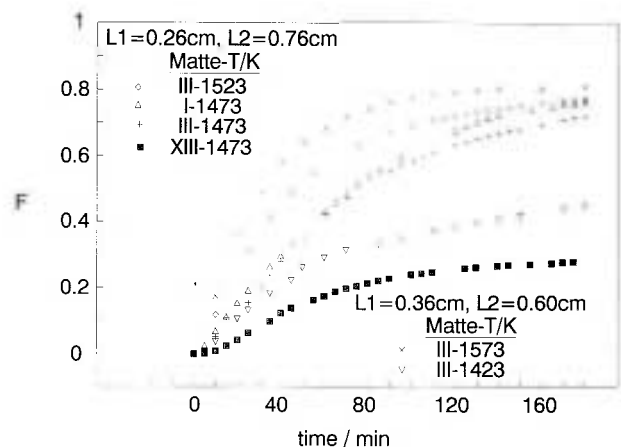


**Figure 4.** Effect of time, temperature, matte composition and boat dimensions on the PbS fractional weight gain.

Table I is demonstrated against the argon flow-rate. The insignificant effect of gas flow-rate (Figure 6) helps to rule-out a varying thickness for the stagnant gas layer.

## RATE OF VAPORIZATION

Assuming the PbS concentration of the gas stream to be negligible, the following partial differential equation and boundary conditions can appropriately describe the system:

$$\frac{\partial C_1}{\partial t} = D_1 \frac{\partial^2 C_1}{\partial y^2} \quad \text{for} \quad 0 \leq y \leq L_1 \quad (4)$$

$$C_1 = (C_1)_0 \quad \text{at} \quad t = 0 \quad (5)$$

$$\frac{\partial C_1}{\partial y} = 0 \quad \text{at} \quad y = 0 \quad (6)$$

$$-D_1 \left( \frac{\partial C_1}{\partial y} \right)_{y=L_1} = \frac{D_g [(C_g)_{y=L_1} - 0]}{L_2 - L_1} \quad (7)$$

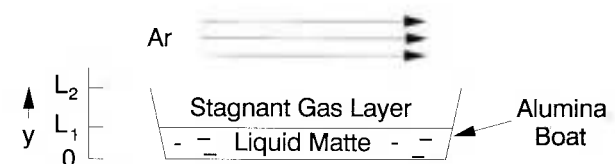


**Figure 5.** Schematic representation of the vaporization system used in this study.

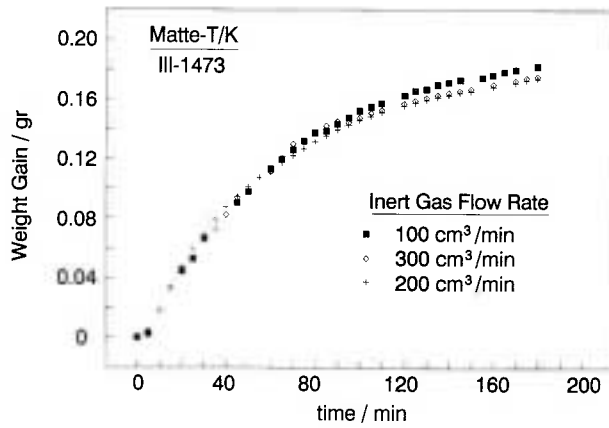


**Figure 6.** Effect of the inert gas flow-rate on the total weight of the species vaporized from Matte III at 1473 K.

$$K_c = \frac{(C_g)_{y=L_1}}{(C_l)_{y=L_1}} \quad (8)$$

$$K = \frac{(P_g)_{y=L_1}}{(a_l)_{y=L_1}} = \frac{(C_g)_{y=L_1} \cdot RT}{\gamma_l (C_l)_{y=L_1} / \rho_l} = \frac{RT \rho_l}{\gamma_l} K_c \quad (9)$$

- $C_l$ : concentration of PbS in the liquid matte  
 $t$ : time  
 $D_l$ : diffusivity of PbS in the liquid matte  
 $y$ : distance from bottom of the boat  
 $(c_l)_0$ : initial concentration of PbS in the matte  
 $L_l$ : depth of the liquid matte  
 $D_g$ : diffusivity of PbS in the gas  
 $C_g$ : concentration of PbS in the gas  
 $L_2$ : total height of the alumina boat  
 $K_c$ : equilibrium concentration ratio  
 $P_g$ : partial pressure of PbS in the gas  
 $a_l$ : activity of PbS in the liquid matte  
 $\gamma_l$ : activity coefficient of PbS in the liquid matte  
 $\rho_l$ : density of the liquid matte  
 $K$ : equilibrium constant for PbS vaporization

It is assumed that there is equilibrium at the liquid/gas interface and that steady state diffusion occurs in the stagnant layer of gas filling the upper empty part of the boat ( $L_2-L_1$  in Figure 5).

Selected standard free energy data is used to

calculate the equilibrium constant  $K$  of the vaporization reaction. The results are given in Table II. The binary inter-diffusivity  $D_g$  used in Equation 7 is estimated from the Chapman-Enskog theory [14]:

$$D_g = \frac{0.0018583 T^{3/2}}{P (\sigma_{Ar-PbS})^2 \Omega_{Ar-PbS}} \sqrt{\frac{1}{M_{Ar}} + \frac{1}{M_{PbS}}} \quad (10)$$

where the collision diameter  $\sigma_{Ar-PbS}$  is taken to be the same as that of Ar and Pb:

$$\sigma_{Ar-PbS} = \frac{1}{2} (\sigma_{Ar} + \sigma_{PbS}) \approx \sigma_{Ar-Pb} = \frac{1}{2} (3.29 + 3.42) = 3.36 \text{ \AA} \quad (11)$$

and the collision integral  $\Omega_{Ar-PbS}$  is determined at dimensionless temperature,  $T^*_{Ar-PbS}$ , for the Lennard-Jones potential [14]:

$$T^*_{Ar-PbS} = \left( \frac{K_B}{\epsilon} \right)_{Ar-PbS} \cdot T \quad (12)$$

The average intermolecular force parameter,  $(\epsilon/K_B)_{Ar-PbS}$ , is

$$\left( \frac{\epsilon}{K_B} \right)_{Ar-PbS} = \sqrt{\left( \frac{\epsilon}{K_B} \right)_{PbS} \cdot \left( \frac{\epsilon}{K_B} \right)_{Ar}} \sqrt{(1.92 T_M)(124)} = 423 \text{ K} \quad (13)$$

in which  $T_M$  is the melting temperature of PbS and is depicted from Reference 15 and other physical data

**TABLE II. Equilibrium-Constant and Inter-diffusivity Data.**

T (°C)	K = P° <sub>PbS</sub> [3,7,8]	Ω <sub>Ar-PbS</sub> [14]	D <sub>g</sub> (cm <sup>2</sup> /S)	D <sub>l</sub> (cm <sup>2</sup> /S)
1115	0.11741	0.90	1.61	1.34X 10 <sup>-5</sup>
1120	0.12396	0.90	1.62	1.37X 10 <sup>-5</sup>
1125	0.13082	0.90	1.63	1.41X 10 <sup>-5</sup>
1140	0.15342	0.89	1.68	1.52X 10 <sup>-5</sup>
1150	0.17030	0.89	1.70	1.60X 10 <sup>-5</sup>
1200	0.28095	0.88	1.81	2.03X 10 <sup>-5</sup>
1210	0.30928	0.88	1.85	2.12X 10 <sup>-5</sup>
1250	0.44846	0.87	1.92	2.53X 10 <sup>-5</sup>
1300	0.69499	0.87	2.02	3.12X 10 <sup>-5</sup>

are depicted from References 14 and 16. The values of inter-diffusivities for different experimental temperatures are summarized in Table II.

Inter-diffusivity correlations of liquids are taken similar to those for solids by many authors [17, 18]. For pseudo-binary  $\text{Cu}_2\text{S}$ -PbS mattes one can write, for example:

$$D_1 = X_{\text{PbS}} D_{\text{Cu}_2\text{S}} + X_{\text{Cu}_2\text{S}} D_{\text{PbS}} \quad (14)$$

in which  $X_{\text{PbS}} \ll 1$  and hence:

$$D_1 = X_{\text{Cu}_2\text{S}} D_{\text{PbS}} \approx D_{\text{PbS}} \quad (15)$$

More complex correlations are available for multi-component systems in the literature [19]. From the widely sparse diffusivity data available in the literature, the molecular diffusion coefficient of PbS is estimated by comparing the thermochemical properties of the molten oxide and sulfide systems of similar compositions [20]. The results are illustrated in Table II.

A detailed discussion of how to solve Equations 4 to 9 is given by Carslaw and Jaeger [21]. The fractional weights of the vaporizing substance obtained from the numerical values of Newmann [22] are illustrated by Crank [23] and Szekely, et al., [24]. They have plotted the fractional weights of the vaporizing substance for different values of parameter  $\beta$  which is the positive root of the following equation:

$$\beta \tan \beta = \lambda \quad (16)$$

in which  $\lambda$  is defined by:

$$\lambda = \frac{K_c L_1 D_g}{(L_2 - L_1) D_1} \quad (17)$$

and the fractional weight of the vaporizing substance

PbS is given by:

$$F = 1 - \sum_{n=1}^{\infty} \frac{2 \lambda^2 e^{-\beta_n^2 D_1 / L_1^2}}{\beta_n^2 (\beta_n^2 + \lambda^2 + \lambda)} \quad (18)$$

Figure 7 shows the fractional vaporization data obtained experimentally and theoretically at different temperatures and matte compositions. The curves are comparable with the numerical solutions plotted by the above authors. The horizontal axis is scaled in terms of the dimension-less quantity defined by Equation 19. From the best match of the data, the closest values of  $\lambda$  and from there the closest figures for  $K_c$  are obtained. These figures are calculated for the initial stages of vaporization when the matte composition has not yet significantly been changed. Using these values, the activity coefficient of PbS is obtained from Equation 20 and is tabulated in Tables III and IV.

$$\theta = \sqrt{\frac{D_1 t}{L_1^2}} \quad (19)$$

$$\gamma_1 = RT \rho_1 \frac{K_c}{K} \quad (20)$$

The variation of the activity coefficient of PbS with both temperature and composition of the matte is described by the following equations which are found from the experimental results:

$$\ln \gamma_{\text{PbS}} = -\frac{4987}{T} + 1.61 \quad \text{for Matte No. I} \quad (21)$$

$$\ln \gamma_{\text{PbS}} = -\frac{4954}{T} + 1.30 \quad \text{for Matte No. III} \quad (22)$$

$$\ln \gamma_{\text{PbS}} = -\frac{4897}{T} + 0.30 \quad \text{for Matte No. XIII} \quad (23)$$

From the slope and the intercept of the  $\ln \gamma_{\text{PbS}}$  vs.  $1/T$  curves, the excess enthalpy and the excess entropy of dissolution of PbS in the liquid mattes of



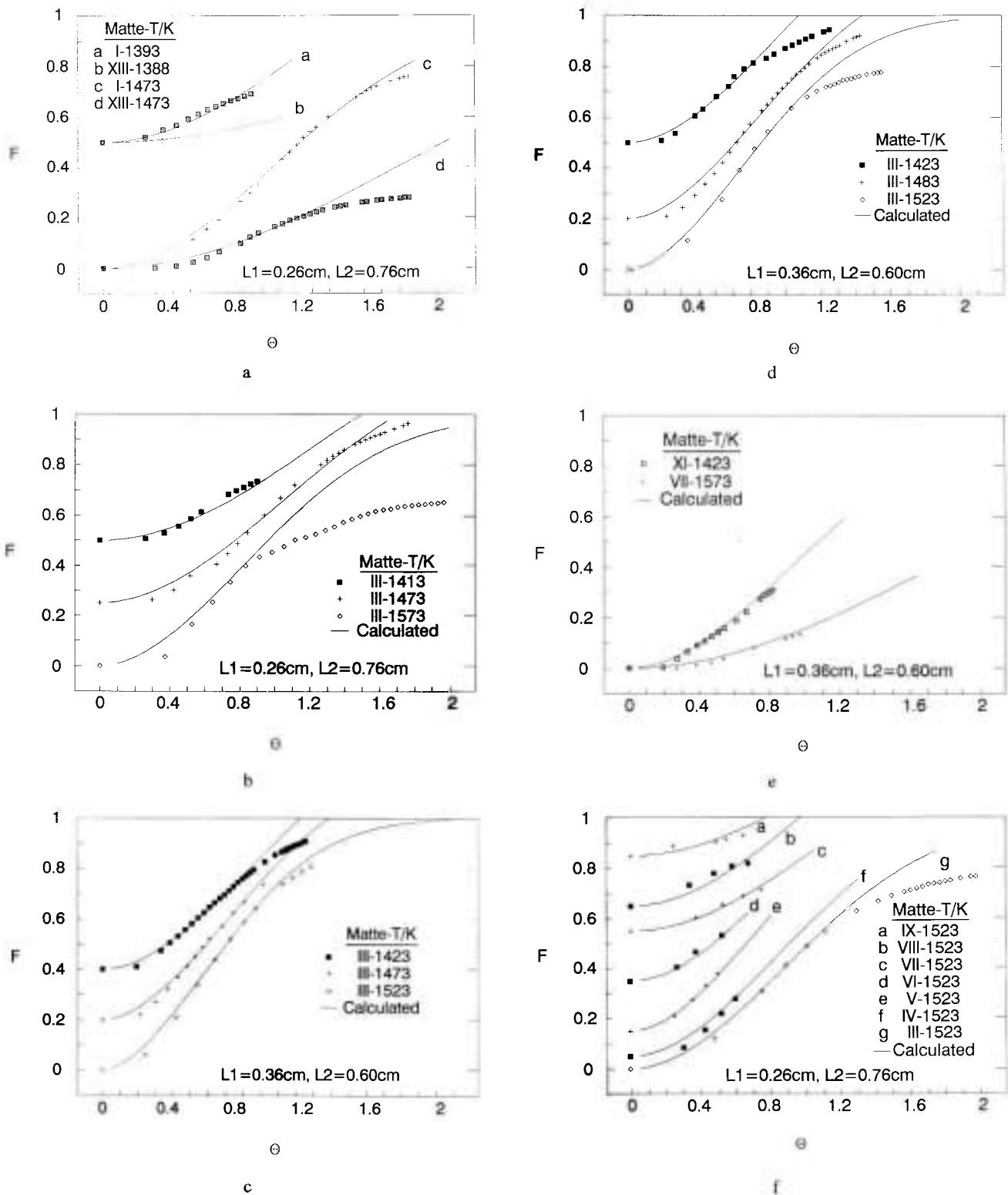


**Figure 7.** A comparison of the theoretical with the experimental fractional vaporization data obtained at different experimental conditions specified in the figure assuming constant PbS activity coefficients. Note that the origin of the vertical axes is shifted for a number of the curves.

**TABLE III. Calculation of the Activity Coefficient of PbS Dissolved in Liquid Mattes of Different Compositions and Temperatures. The values are determined for the initial stages of vaporization when %PbS=3.**

T (°C)	Matte	$\frac{L_1}{L_2 - L_1}$	$\lambda$	$K_c$	$\gamma_i$
1120	I	0.52	0.37	$6.017 \times 10^{-6}$	0.1468
1200	I	0.52	0.65	$1.402 \times 10^{-5}$	0.1595
1140	III	0.52	0.35	$6.090 \times 10^{-6}$	0.1217
1150	III	1.50	0.90	$5.647 \times 10^{-6}$	0.1024
1150	III	1.50	0.95	$6.961 \times 10^{-6}$	0.1081
1150	III	1.50	0.95	$6.961 \times 10^{-6}$	0.1081
1200	III	0.52	0.57	$1.229 \times 10^{-5}$	0.1399
1200	III	1.50	1.70	$1.271 \times 10^{-5}$	0.1447
1200	III	1.50	1.45	$1.084 \times 10^{-5}$	0.1234
1210	III	1.50	1.35	$1.031 \times 10^{-5}$	0.1073
1250	III	1.50	2.50	$2.196 \times 10^{-5}$	0.1619
1250	III	1.50	1.90	$1.669 \times 10^{-5}$	0.1230
1250	III	0.52	0.85	$2.154 \times 10^{-5}$	0.1588
1300	III	0.52	1.00	$2.970 \times 10^{-5}$	0.1459
1300	III	1.50	2.90	$2.986 \times 10^{-5}$	0.1467
1115	XIII	0.52	0.10	$1.601 \times 10^{-6}$	0.0411
1200	XIII	0.52	0.19	$4.098 \times 10^{-6}$	0.0466

**TABLE IV. Calculation of the Activity Coefficient of PbS Dissolved in Liquid Mattes of Different Initial PbS Concentrations. Other compositions are given in Table I.**

T (°C)	%PbS	Matte	$\frac{L_1}{L_2 - L_1}$	$\lambda$	$K_c$	$\gamma_i$
1150	1.25	XI	1.50	0.75	$1.052 \times 10^{-6}$	0.0854
1250	2.40	IV	0.52	0.95	$1.702 \times 10^{-5}$	0.1775
1250	1.91	V	0.52	1.40	$1.943 \times 10^{-5}$	0.2615
1250	1.60	VI	0.52	0.90	$1.903 \times 10^{-5}$	0.1681
1250	1.10	VII	0.52	0.40	$1.803 \times 10^{-5}$	0.0747
1250	0.90	VIII	0.52	0.54	$1.702 \times 10^{-5}$	0.1009
1300	1.10	VII	1.50	0.15	$9.900 \times 10^{-6}$	0.0065

this study are evaluated. The results are given in Table V.

## DISCUSSION

The kinetic model described in this paper is used to calculate the fractional vaporization from various liquid mattes of this investigation. The calculated fractional vaporization ( $F_c$ ) must fit with the experi-

mental ones ( $F_E$ ). A criterion for determination of the fitness is defined by Equation 24:

$$\delta = \sqrt{\sum_{i=1}^n (F_c - F_E)^2 \theta} \quad (24)$$

in which minimization of the quantity,  $\delta$ , can lead to the most appropriate coefficient.

Examples of the calculated versus measured fractional vaporizations are demonstrated in Figure 7.

**TABLE V. Excess Enthalpies and Excess Entropies of Dissolution of PbS in Cu<sub>2</sub>S-FeS-PbS Mattes.**

Matte	X <sub>PbS</sub>	ΔH <sub>PbS</sub> <sup>E</sup> (J/.mol)	ΔS <sub>PbS</sub> <sup>E</sup> (J/K.mol)
I	0.014	-41462	-13.39
III	0.015	-41188	-10.81
XIII	0.020	-40714	-2.49

The calculated values are almost in all cases satisfactorily consistent with the experimental data. Minor deviations are, however, observed at lower times when the steady state vaporization conditions are not fully developed yet, and at greater times when the concentration of PbS falls substantially below its initial value. The former difference can simply be described by the heating and the melting processes that must initially occur in the system. The latter indicates that the higher initial concentrations can not be assumed in the range of Henry's law behavior with a constant activity coefficient of PbS in the system. This latter conclusion contradicts the assumption made by many authors about the Henrian behavior of the concentrated complex matte systems.

If, for example, the initial concentration of PbS is outside the range of Henry's law behavior and with the negative deviation from ideality of PbS, as is indicated in Tables III and IV, the continuation of the vaporization process lowers both the PbS concentration and the value X<sub>1</sub> during a continued vaporization test. A comparison of the activity coefficients obtained for similar mattes of different initial PbS concentrations such as mattes III, IV, V, VI, VII and VIII of Tables III and IV can also be taken as a proof for this conclusion.

For a general condition of non-Henrian behavior, different amounts of λ's are utilized through a computer program to find the best matching activity coefficients (Figures 8a and 8b). the values obtained through this procedure are functions of both matte composition and temperature. Calculations show that

the effect of slight variations in such properties as ρ<sub>1</sub> and D<sub>1</sub> is negligible.

From Figures 2 and 3, a pull-out solidification of the matte causes an obvious initial change in the rate of vaporization of the melt. Repeated experiments on a room temperature holding of more than twenty four hours has shown almost the same effect as a 600°C annealing of ten, five or even three minutes. The new curves all consistently fit with the three-stage model described here. It can, therefore, be concluded that the forced mixing homogenization due to the pull-out solidification can cause the creation of a new matte from a previously partially extracted melt.

The negative values of ΔH<sub>PbS</sub><sup>E</sup> and ΔS<sub>PbS</sub><sup>E</sup> show that the dissolution of PbS in all liquid mattes causes a

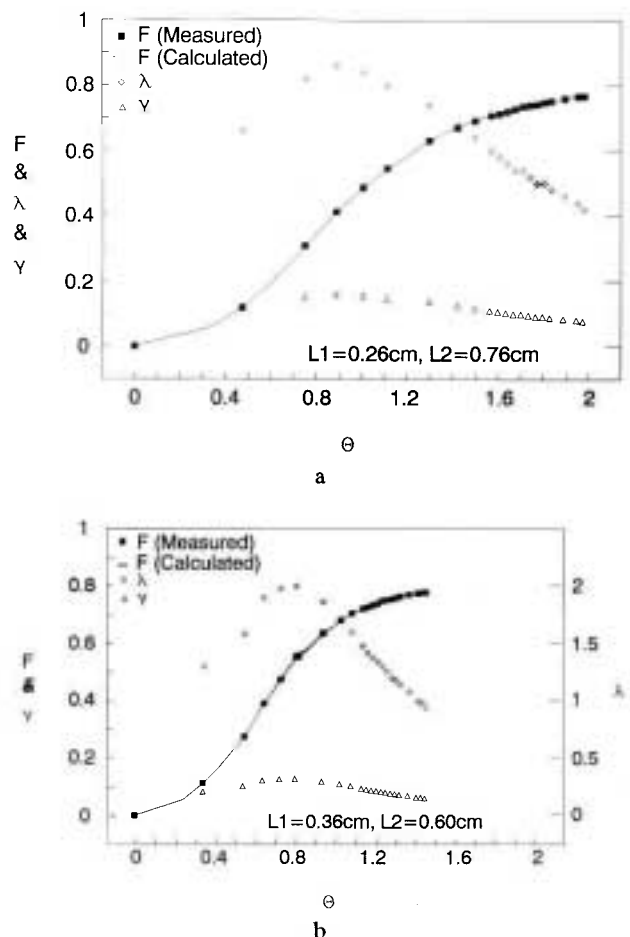


**Figure 8.** Calculated vs. measured vaporization data for matte III at 1250°C assuming variable activity coefficients.

reduction in the volume of the system [15] and a liberation of energy and entropy. These findings are consistent with the previously obtained empirical linear relationship on the maximum or minimum of the excess extensive quantities of the liquid metal/semi-metal binary alloys [25] with covalent bonds [26,27]. The relatively large value of  $-\Delta S_{\text{PbS}}^E$  indicates the tendency of the sulfide molecular species to cluster [28] and that all the mattes are unlikely to obey a regular solution model.

The decrease in  $-\Delta S_{\text{PbS}}^E$  from matte I to matte XIII indicates that the PbS dissolves less ideally in  $\text{Cu}_2\text{S}$ -FeS than in  $\text{Cu}_2\text{S}$  mattes. A comparison of the molecular geometry and specific conductance of FeS, PbS and  $\text{Cu}_2\text{S}$  [29,30] shows that the similarity between the first two is greater than that between the last. This may be due to the alterations in the vibrational entropy which is accompanied by a reduction of the specific volume of PbS; and to vibrational ordering, which can be attributed to the polar bonds between Pb and S. The negative excess entropy of dissolution of PbS is apparently due to the partial polar forces in the  $\text{Cu}_2\text{S}$ -FeS melts that consist partly of  $\text{Pb}^{2+}$ ,  $\text{S}^{2-}$ ,  $\text{Cu}^+$  and  $\text{Fe}^{2+}$  ions. Basically these forces exert their influence on the vibrational entropy terms.

### SUMMARY

A modification of the conventional transportation technique is used to determine the thermodynamics and the kinetics of vaporization of lead sulfide from complex Cu-Fe mattes. The content at time  $t$  of PbS in the matte is obtained by subtracting the vaporized amount from the initial value. The vaporized amount is calculated from the weight and chemical analysis of the condensed materials.

The rate of vaporization of PbS is simply determined from the weight gain and from analysis of the

materials captured through condensation. It is found that this can be a successful method for producing reliable data in highly corrosive environments simulating Cu-Fe smelting and converting systems.

From among many kinetic equations available, a vaporization model based on three consecutive steps of 1) diffusion in the liquid, 2) equilibrium at the interface and 3) diffusive transfer in the gas, has proved to appropriately describe the PbS vaporization system.

Application of Equations 3 to 18 to the vaporization of PbS from Cu-Fe mattes shows that there is an acceptable match between the experimental and the calculated data (Figure 8a and 8b). The experimental results are further utilized to calculate the activity and the activity coefficient of PbS. Based on these results, Equations 21, 22 and 23 are obtained for activity coefficient of PbS versus temperature.

### ACKNOWLEDGEMENTS

The proposal for this research was first designed by Late Professor John F. Elliott of MIT who passed away in April 1991. The author wishes to acknowledge his initiation, his initial leadership and his partial financial support of the work when the author was a visiting scientist at MIT. The author also wishes to acknowledge the financial support received afterwards from the Sharif University of Technology at Tehran, I. R. Iran for continuation of the study.

### REFERENCE

1. C. B. Alcock and G. W. Hooper, "Measurement of Vapor Pressures at High Temperatures by the Transportation Method": *Phys. Chem. of Process Metallurgy*, Part 1, (1959), 325-340.

2. U. Merten, "Diffusion Effects in the Transpiration Method of Vapor Pressure Measurement": *J. Phys. Chem.*, Vol. 63, (1959), 443-445.
3. V. N. Nesterov, R. A. Isakova and A. S. Shendyapin, "The Activity of Lead in Sulphide Melts": *Russ. J. Phys. Chem.*, 43, (12), (1969), 1785-1787.
4. K. Azuma, S. Goto and N. Takabe: *Nippon Kogyo Kaishi*, 86, (1970), 35-40 (Cited by Ref. 7).
5. M. Nagamori and P. J. Mackay, "Thermodynamics of Copper Matte Converting": *Metallurgical Transactions B*, 9B, (1978), 567-579.
6. S. N. Sinha and M. Nagamori, "Activities of CoS and FeS in Copper Mattes and the Behavior of Cobalt in Copper Smelting": *Metallurgical Transactions B*, 13B, (1982), 461-470.
7. H. Eric and M. Timucin, "Activities in  $Cu_2S$ -FeS-PbS Melts at 1200°C": *Metallurgical Transactions B*, 12B, (1981), 493-500.
8. S. N. Sinha, H. Y. Sohn and M. Nagamori, "Distribution of Lead between Copper and Matte and the Activity of PbS in Copper-Saturated Mattes": *Metallurgical Transactions B*, 15B, (1984), 441-449.
9. R. Colin and J. Drowart, "Thermodynamic Study of Tin Sulfide and Lead Sulfide Using a Mass Spectrometer": *J. Chem. Phys.*, 37, (1962), 1120-1125.
10. A. Roine, "Activities of As, Sb, Bi, and Pb in Copper Mattes-Impurity Elimination": *Metallurgical Transactions B*, 18B, (1987), 213-223.
11. A. Roine and H. Jalkanen, "Activities of As, Sb, Bi and Pb in Copper Mattes": *Metallurgical Transactions B*, 16B, (1985), 129-141.
12. El-Rahaiby and Rao, "Kinetics of Vaporization of Lead Sulfide": *Metallurgical Transactions B*, 13B, (1982), 633-641.
13. Y. A. Chang, J. P. Neumann and U. V. Choudary, "Phase Diagrams and Thermodynamic Properties of Ternary Copper-Sulfur-Metal Systems", (International Copper Research Association, NSRDS, 1979), 73.
14. G. H. Geiger and D. R. Poirier, "Transport Phenomena in Metallurgy", (Addison-Wesley, 1973), 464-466.
15. O. Kubaschewski and C. B. Alcock, "Metallurgical Thermo-chemistry", 5th Ed., (Pergamon Press, 1979).
16. F. D. Richardson, "Physical Chemistry of Melts in Metallurgy", Vol. 1, (Academic Press Inc., 1974), 62.
17. T. Lotlin and E. Mclaughlin, "Diffusion in Binary Liquid Mixtures": *J. Phys. Chem.*, 73, (1969), 186.
18. P. C. Carman: *J. Phys. Chem.*, 71, (1967), 2565.
19. T. K. Kett and D. K. Anderson, "Multicomponent Diffusion in Nonassociating, Nonelectrolyte Solutions": *J. Phys. Chem.*, 73, (1969), 1262.
20. J. F. Elliott, M. Gleiser and V. Ramakrishna, "Thermo-chemistry for Steelmaking", Vol. I and Vol. II, Addison-Wesley, Mass., (1960 and 1963).
21. H. S. Carslaw and J. C. Jaeger, "Conduction of Heat in Solids", (Oxford University Press, 1947), 252.
22. A. B. Newman, "The Drying of Porous Solids: Diffusion Calculations": *Trans. Amer. Inst. Chem. Engrs.*, 27, (1931), 203.
23. J. Crank, "The Mathematics of Diffusion", (Oxford University Press, 1970), 57.
24. J. Szekely and N. J. Themelis, "Rate Phenomena in Process Metallurgy", (John Wiley & Sons, 1971), 403.
25. A. A. Briggs, W. A. Dench and W. Slough, "Null-Point Solid Electrolyte Electrochemical Cell for Measuring Low Oxygen Partial Pressures at High Temperatures", *J. Chem. Thermodyn.*, 3, 1, (1971), 43-49.
26. O. Kubaschewski, "The Change of Entropy, Volume and Binding State of the Elements on Melting", *Trans. of Faraday Soc.*, 45, (1949), 931-946.
27. O. Kubaschewski and R. Hornle, "Densities of Liquid  $Mg_2Pb$  and  $Mg_3Bi_2$ ", *Z. Metallurgica*, 42, (1951), 129.
28. C. B. Alcock and F. D. Richardson, "Dilute Solutions in Alloys": *ACTA Metallurgica*, 8 (1960), 882-887.
29. D. Richardson, "Physical Chemistry of Melts in Metallurgy", Vols. 1&2, (Academic Press, 1974).
30. E. A. Cancy and G. Derge, "Electrical Conductivity of the Molten Co-S, Ni-S, and Ag-S Systems", *J. Trans. A.I.M.E.*, 227, (1963), 1034.